AAS 17-695 PATCHED PERIODIC ORBITS: A SYSTEMATIC STRATEGY FOR LOW ENERGY TRANSFER DESIGN

Conference Paper · August 2017

CITATIONS
9

READS
660

2 authors:

Ricardo L. Restrepo
University of Texas at Austin
9 PUBLICATIONS **90** CITATIONS
SEE PROFILE

Ryan P. Russell
University of Texas at Austin
191 PUBLICATIONS **3,417** CITATIONS
SEE PROFILE

AAS 17-695

PATCHED PERIODIC ORBITS: A SYSTEMATIC STRATEGY FOR LOW ENERGY TRANSFER DESIGN

Ricardo L. Restrepo* **and Ryan P. Russell†**

The design of low energy transfers is in general a tedious, time consuming task due to the high dynamical complexity of multi-body environments. A new systematic strategy, which seeks to ease the complexity of this task, is presented. In this model, we show how precomputed three-body periodic orbits can be patched together to give rise to complex trajectories. The patched periodic orbits in the restricted three body problem is analogous to the patched conics of the two body problem. The work focuses on the design of capture and escape trajectories, as well as transfers around the minor body of the three-body system. Several examples are presented, with emphasis on the Jupiter-Europa and Earth-Moon systems.

INTRODUCTION

The latest developments in dynamical system theory have been applied to the design of complex trajectories in multi-body environments, leading to some of the ultimate techniques in astrodynamics .[1,2,3,4] These techniques are especially useful in the computation of orbit transfers in low energy regimes, where the patched-conic approximation loses its validity. Dynamical system theory has helped unveil the existence of natural transport mechanisms, where trajectories follow the natural flows of the third-body perturbed systems, hence, opening a new world of routes for space exploration. In the Earth-Moon system, missions such as ARTEMIS[5] and Genesis[6] have successfully implemented these techniques. Currently, Europa and Enceladus are of high scientific interest due to their potential to harbour life, and low energy trajectories enable efficient access to them.[7] A main disadvantage of low-energy trajectory design is the complexity of the large design space and chaotic dynamics. The goal of this paper is to provide a systematic strategy to ease the complex work of designing these types of trajectories.

A classic example of a complex low energy design is found in the "Petit Grand Tour", Tour?, an idea first presented by.[8] This approach is infeasible using conventional patched conics and provides free temporary captures, allowing for more science collection than the typical high energy moon tours. In general, in a low energy moon tour design, a single orbiter navigates through the natural satellites of a planetary system (e.g., the Galilean moons), looping around them at each encounter, all of this designed with minimum fuel consumption. The moon tour problem is typically de-coupled in two phases: the transfer between adjacent moons, and the capture/escape transition. Ballistic

*Graduate Student, Department of Aerospace Engineering and Engineering Mechanics, The University of Texas at Austin, W.R. Woolrich Laboratories, C0600. 210 East 24th Street, Austin TX 78712-1221; ricardo.rpo@utexas.edu.

†Associate Professor, Department of Aerospace Engineering and Engineering Mechanics, The University of Texas at Austin, W.R. Woolrich Laboratories, C0600. 210 East 24th Street, Austin TX 78712-1221; ryan.russell@utexas.edu

transfers between moons are possible via resonant hopping sequences.[9] Resonant hopping design has been addressed by several authors and multiple strategies have been investigated.[10,11,12]

The current study is focused on the capture/escape phase and the motion of the spacecraft around the minor bodies. These transfers are dominated by chaotic dynamics and their design typically involved the computation of invariant manifolds of unstable periodic orbits in 3-body dynamics.[2,13,14,15] The invariant manifolds form a transportation tube network[16] that provides natural transitions between libration point orbits, resonant orbits, and weak captured orbits. However, this approach requires the computation of a large number of manifolds and finding their intersections. What we propose here is a different, less computationally expensive mechanism to build these transportation networks. The model, called *Patched Periodic Orbits* (PPO), is analogous to the patched conic model in the 2-body problem, when conic segments are used as building blocks, which are patched together to give rise to full complex trajectories. In our case, the building blocks are precomputed 3-body periodic orbits (POs), which are then simply patched together to build transfer mechanisms in multi-body environments, therefore reducing the complexity of the process.

The selected periodic orbits used in the PPO model and all the examples reported in this paper are obtained from a catalog of 3-body POs provided by the authors and available online.[17] The catalog includes an extensive set of families of planar x-axis symmetry periodic orbits for the principal bodies of the Solar System, i.e., sun-planet and planet-moon systems. Reference 17 provides a detailed description of the families in the catalog and its generation strategy. The catalog also includes a set of parameters that allow for easy identification and classification of the families (e.g., stability index and Jacobi constant), providing the necessary framework for the PPO model. Simple periodic orbits around the equilibrium points L_1 and L_2 (e.g. Lyapunovs orbits), together with prograde orbits around the minor body, are used as loose captured orbits or temporary *stations*. These loitering orbits are POs that naturally patch together more complicated periodic orbits. Ballistic transfers between these loitering orbits, known as heteroclinic connections, are approximated by a special set of periodic orbits. An additional group of POs are used to patch loose captured orbits with inner and outer resonant orbits leading to the escape/capture trajectories that transition to the inter-moon phase.

The paper is organized as follows. First, background is presented on the restricted 3-body problem and the theory relevant to the model. The next section describes the PPO model in detail, including the description of two different strategies to patch a sequence of POs. Next a description is provided of how to use the PPO model to design escape and capture trajectories, and transfers in the vicinity of the minor body. Several examples in different systems are then presented, and conclusions are drawn.

BACKGROUND

The Patched Periodic Orbit model is developed as a straightforward mechanism to design low energy transfer trajectories in the Circular Restricted 3-Body Problem (CR3BP) and multi-body environments. In this section we briefly review the CRTBP and some of its properties relevant to this work.

The Circular Restricted 3-Body Problem

In the CR3BP the motion of a test particle of non-thrusting spacecraft is governed by the gravity of two bodies $B1$ and $B2$ moving in circular orbits around their barycenter.[18] Using dimension-

less units in a rotating, barycentric frame, the equations of motion of the spacecraft with position coordinates x, y, and z, are given by

$$\begin{cases} \ddot{x} - 2\dot{y} &= \partial\Omega/\partial x \\ \ddot{y} + 2\dot{x} &= \partial\Omega/\partial y \\ \ddot{z} &= \partial\Omega/\partial z \end{cases} \tag{1}$$

where the potential

$$\Omega = \frac{x^2 + y^2}{2} + \frac{1-\mu}{r_1} + \frac{\mu}{r_2} \tag{2}$$

and $r_1 = \sqrt{(x+\mu)^2 + y^2 + z^2}$ and $r_2 = \sqrt{(x-1+\mu)^2 + y^2 + z^2}$ are the distances to the primary ($B1$) and the secondary ($B2$), respectively. The mass parameter μ is defined as $\mu = m_2/(m_1 + m_2)$, where m_1 and m_2 are the masses associated to the primary and the secondary. In the barycentric frame, the primary is located a $x = -\mu$, and the secondary at $x = 1 - \mu$. The x-axis of the rotating frame is aligned with the main bodies, the y-axis points in the direction of motion of the secondary, and the z-axis completes the right-handed coordinate frame.

The CR3BP exhibits one integral of motion, the Jacobi constant J

$$J = 2\Omega - v^2 = x^2 + y^2 + \frac{2(1-\mu)}{r_1} + \frac{2\mu}{r_2} - v^2 \tag{3}$$

where $v = \sqrt{\dot{x}^2 - \dot{y}^2 - \dot{z}^2}$ is the velocity of the spacecraft in the rotating frame. The Jacobi constant is a measure of the energy of the spacecraft and cannot be changed unless a maneuver is applied. High Jacobi constant is equivalent to low energy and high energy is equivalent to low Jacobi constant. There are five equilibrium points in the CR3BP, the Lagrangian points $L_i, i = 1, ..., 5$, with three collinear points located along $y = 0$, and two triangular equilibrium points located at the same distance from the primary as from the secondary. In general, the equilateral points are stable while the collinear point are unstable. The value J_{L_i} is the Jacobi constant of a stationary particle located at the equilibrium point i.

Periodic orbits (POs) exist in the CR3BP. Their center of motion can be the primary, the secondary, the equilibrium points, or a combination of these with an infinite variety of itineraries.[1] The periodic orbits can be stable or unstable, and their stability plays an important role in the process of trajectory design. In particular, the unstable POs are key elements in low energy transfer mechanisms.

Low Energy Regime

The Jacobi constant is useful for a variety of applications in trajectory design. One of these applications is the definition of regions of motion and forbidden zones, which are bounded by a surface called *zero velocity curves* or ZVC (see Figure 1). For a given Jacobi constant there are regions where the spacecraft is allowed, and other regions where the spacecraft's energy prohibit access. For instance, if the Jacobi constant is bigger than J_{L_1}, the ZVC forms a donut shape along the secondary's path of motion. This ZVC divides the space in an inner and outer region where motion is possible, but transitions from one to another are not. At this energy level, the secondary is also isolated from these two regions, and therefore, bounded trajectories around the secondary will remain there indefinitely. In this scenario, the spacecraft is in a "very" low energy regime. If the energy is slightly increased ($J < J_{L_2}$)* a small opening (neck) in the vicinity of the secondary

*Note, $J_{L_2} \approx J_{L_1}$ for small μ.

appears as can be observed in Figure 1. The neck is referred to as a dynamical channel, which allows transfers between the inner and outer regions. In this scenario the spacecraft is considered to be in a low energy regime, which is the energy level of interest for this paper. If the energy is increased such that $J < J_{L_3}$, the spacecraft possesses an excess velocity with respect to $B2$ (in a two-body sense), and consequently, bounded trajectories around the secondary are not possible.[11] The spacecraft is said to be in a high energy regime. The Jacobi constant $J = J_{L_3}$ defines the upper limit of low energy regime, which can now be fully characterised by $J_{L3} < J < J_{L2}$.

In the low energy regime, the region around the secondary exhibits chaotic behavior. Thus, small perturbations on a trajectory will produce big changes. This high sensitivity is caused by the instability of the region. For example, a particle orbiting L_1 or L_2, can drastically change its course wether it be in the direction of the primary, towards the secondary, or leave to the outer region, just by the effect of an infinitesimal perturbation. This behavior can be undesirable in certain cases, but can also be taken in favor of the design, since it allows for an inexpensive control with a wide range of destinations. Figure 1 shows L_1 and L_2 as the gateways to the dynamical channel. The diagram depicts the natural flow of the dynamics in the vicinity of the secondary. Navigating in this flow, instead of fighting it with thrusting, allows for quasi-ballistic transfers between different regions with complex itineraries, including temporary or weak captures around the secondary, L_1, or L_2.

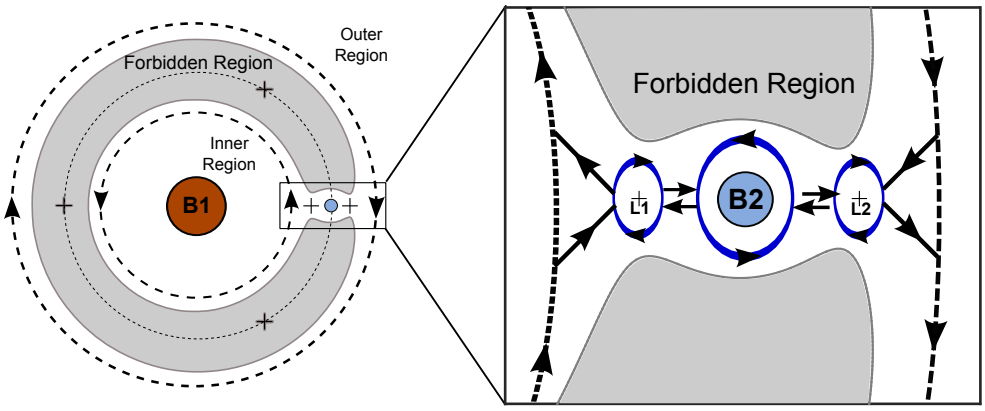

Figure 1. CR3BP diagram for low energy regime. Motion flow direction indicated by arrows

Heteroclinic Connections

The traditional way of designing low energy transfer trajectories is by the use of invariant manifolds, tubes that leave (unstable) and arrive (stable) to and from unstable periodic orbits. When the unstable manifold of a PO intersects with the stable manifold of another PO, it creates a free transport system between the two periodic orbits, called a heteroclinic connection.[19,20] By chaining multiple of these connections, complex trajectories with multiple temporary stations can be created. This procedure is usually tedious, computationally expensive, and time consuming. The present work offers an alternative method, where heteroclinic connections are approximated by a special set of periodic orbits, and are described in detail in the POs database section.

The *Conley-Moser Conditions*. This theorem states that a combination of itineraries with motion around the primary (inner or outer), the secondary, L_1, or L_2 exist with an arbitrary number of revs at each centre of motion.[1] The PPO model provides the means to generate numerical manifestations of this theorem.

PATCHED PERIODIC ORBITS

The high complexity of low energy transfer design is addressed by the development of a systematic method where basic blocks are simply connected together to give rise to complex structures. By selecting a compatible periodic orbit sequence and patching them in a strategic way, complex quasi-ballistc transfers can be designed while reducing the complexity of the process. This model is called Patched Periodic Orbits (PPO) and is presented in this section.

Figure 2 shows an example in the Jupiter-Europa system, where a spacecraft, initially in a outer resonance with Europa, is weakly captured around L_2, where it stays for a few revs before transitioning to L_1. After another few revs around L_1, the spacecraft falls towards the surface of the icy moon, leading to a low orbit capture or landing. The trajectory is obtained by connecting five segments of precomputed periodic orbits (s1–s5), where small maneuvers (Δv) are placed at the patching points. This special trajectory is achieved at the cost of only a few meters per second, and represents both the simplicity and the applicability of the PPO model.

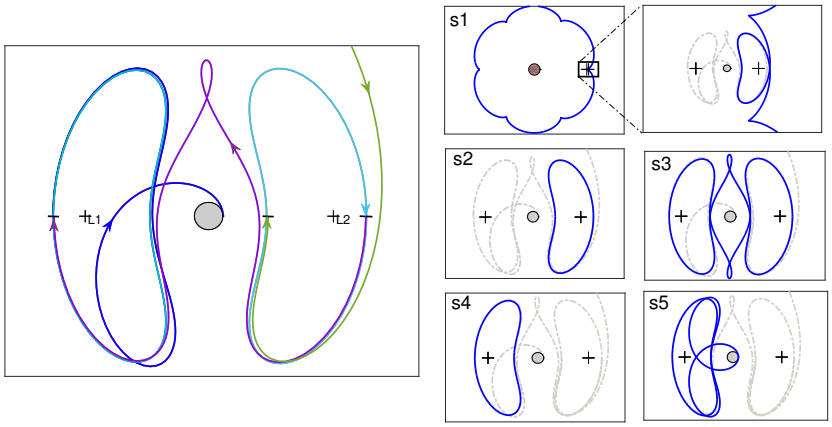

Figure 2. Patched Periodic Orbits example: Outer resonant capture with transition around L_1 and L_2, ending at the Europa surface.

The PPO model consists of two parts: first, a database of precomputed POs, and second, a method to efficiently query the database and to patch the relevant POs together. A final delta-v optimization step can be performed to ensure exact continuity in the final design to if the designer has access to a high fidelity optimization tool; However, provided a well-populated PO database, the method is useful for preliminary design even without a final optimization step.

POs database

The building blocks of the PPO model are periodic orbits. In a previous work, the authors generated a database of planar 3-body periodic orbits for the main bodies of the solar system, and made this database available online.[17] The model is currently restricted to the plane, but it still provides good applicability for moon tour design, Earth-Moon transfers, and motion of minor bodies and other objects in the solar system. The POs used in the model are axisymmetric about the x-axis and are generated with initial conditions on the positive x-axis of the rotating frame. Thus, POs with center of motion around L_3, L_4 and L_5 are not included. x-axisymmetric POs have two perpendicular crossings on the x-axis.[21] It is convenient to patch them at their perpendicular crossing, since

only a $\Delta\dot{y}$ maneuver will be required to generate a continuous trajectory.

A vast literature about the different families of POs in the CRTBP exist. The subset of POs provided in the database is classified in two main groups: 1) POs that are bounded to the secondary body, i.e., never leave its sphere of influence, are referred to in this paper as *bounded* POs or BPOs. 2) Periodic orbits that leave the secondary and cross the negative x-axis fall under the category of *resonant* Periodic Orbits, or RPOs.

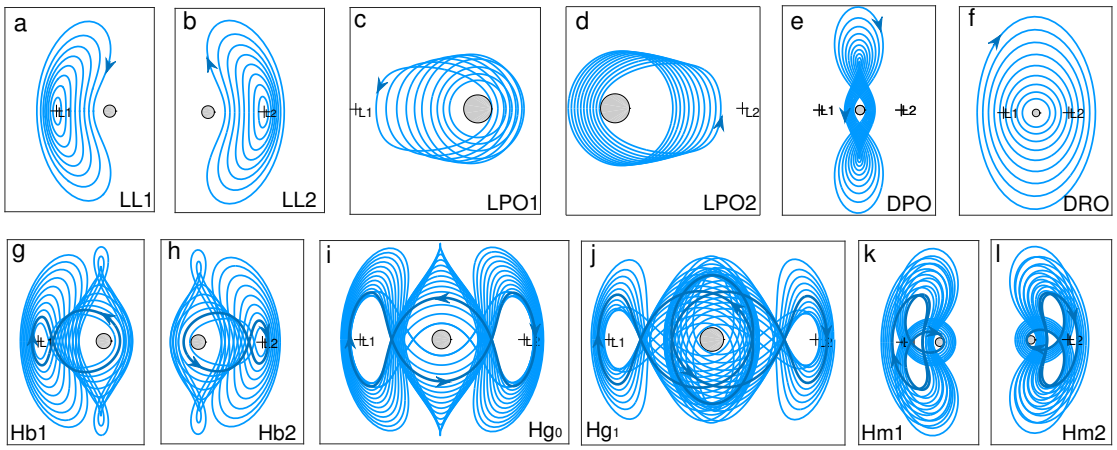

Figure 3. Selected bounded POs: a) to f) *simple* BPOs, h) to j) *composed* BPOs, k) and l) *extended* BPOs

A selected subset of BPOs are part of the *basic building blocks* of the PPO model. This subset is presented in Figure 3 (Jupiter-Europa system) and are the pieces used to build transfers in the vicinity of the secondary. Figure 3(a)–(f) are families with one center of motion and two x-crossings, and represent the most fundamental of the bounded POs (*basic* BPOs). Figure 3(g)–(j) are bounded periodic orbits with multiple centers of motion, called *composed* BPOs, and are used to approximate heteroclinic connections between the basic BPOs. Notice that the composed BPOs can be generated from the basic BPOs through the computation of manifolds and their intersections. This procedure has traditionally been used to compute these highly sensitive families, as shown in Ref. 22 . In our case, that procedure is no longer required and composed BPOs are used instead. Figure 3(k) and (i) are two additional families that do not follow the previous classification but are useful for specific applications and are described later.

From the basic BPOs, Figure 3(a)–(f), the ones orbiting the Lagrangian points L_1 or L_2, are called Lyapunov orbits, and we refer to them as LL_1 and LL_2, respectively. Basic bounded POs orbiting the secondary exist with prograde and retrograde motion. Two stable prograde families are LPO_1 and LPO_2, acronyms that stand for *Low Prograde Orbits*., and are equivalent to Robin and Markellos' g1 and g2 families,[23] and Brouke's H1 and H2 family.[24] The third family of prograde orbits is the *Distant Prograde Orbits* or DPO*. This family is a continuation of the LPO_2 family, which begins in the transition to instability[17] *Distant retrograde orbits* (DRO) are highly stable and quasi-ballistic transfers to and from DROs are not possible. Due to the high transfer cost, retrograde orbit transfers are not included in the present work; however similar strategies to the PPO model can still be implemented.

*These prograde orbits have been historically known as "the g family".[25]

The composed BPOs Hb_1 and Hb_2 are equivalent to Henón's Hb and Hb' orbits.[26] The Hb_1 family approximates heteroclinic connections between LL_1 and LPO_1 as well as LL_1 and DPO (Figure 3(f)). The Hb_2 family approximates heteroclinic connections between LL_2 and LPO_2 as well as LL_2 and DPO (Figure 3(g)). The Hg_0 family, equivalent to Henón's g_3 family, approximates heteroclinic connections between L_1 and L_2 (Figure 3(h)). Connections of this same type, but with multiple number of revolutions around the secondary also exist, which agrees with the Conley-Moser theorem. We label these families as Hg_n, where n represents the number of revs around the secondary. A trajectory with $n = 1$ is shown in Figure 3(i), and a more detailed example with $n = 0, ..., 5$ is shown in Figure 4, where each PO is propagated for only half a period to show the L_1 to L_2 transfer direction. As the number of revs around the secondary increases, the sensitivity of this type of periodic orbit increases, making them numerically difficult to compute.

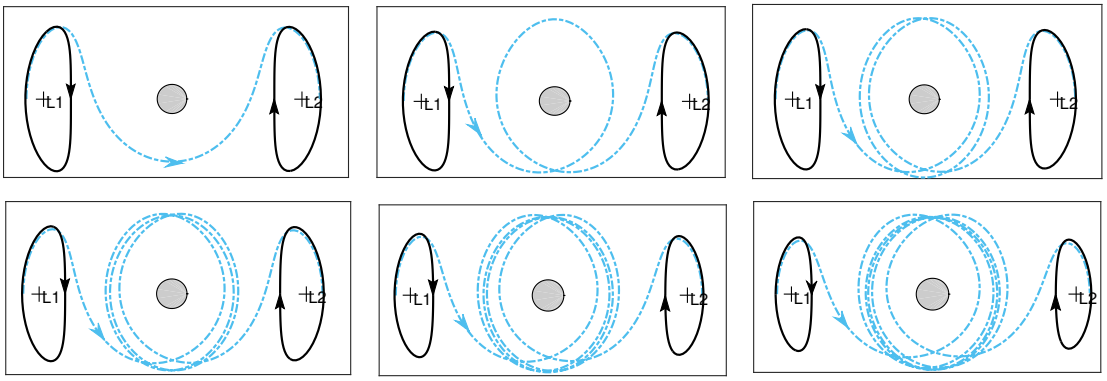

Figure 4. Sample of families Hg_0,..., Hg_5 (light blue): POs that connect L1 and L2 approximating Heteroclinic connections. Lyapunov orbits around L_1 and L_2 (black)

Symbolic Representation

A transfer trajectory composed by a POs sequence can be described by using symbolic representation. For example, a transfer between an L_2 Lyapunov orbit and a distance prograde orbit, patched throughout an Hb_2 PO, is represented as $LL_2 \rightarrow Hb_2 \rightarrow DPO$. This transfer is depicted in Figure 5.a. The methods to patch the POs are described next, with several examples explained in detail (see Table 1).

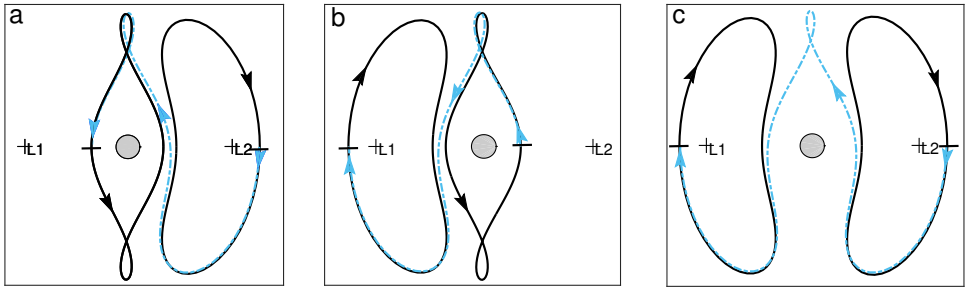

Figure 5. POs sequences for the transfers: a) LL_2 to DPO, b) DPO to LL_1, c) LL_1 to LL_2 . Jupiter-Europa system. $J = (J_{L3} + J_{L2})/2 \approx 3.0018$ (example 1)

Example	Sequence	Figure
ex. 1.a	$LL_2 \rightarrow Hb_2 \rightarrow DPO$	Figure 5.a
ex. 1.b	$DPO \rightarrow Hb_1 \rightarrow LL_1$	Figure 5.b
ex. 1.c	$LL_2 \rightarrow Hg_0 \rightarrow LL_1$	Figure 5.c
ex. 2.a-2.f	$LL_2 \rightarrow Hb_2 \rightarrow DPO$	Figure 7.a-7.f
ex. 3.a1-3.a3	$LL_2 \rightarrow Hb_2 \rightarrow LPO$	Figure 7.a1- 7a.3
ex. 3.b1-3.b3	$LL_2 \rightarrow Hb_2 \rightarrow DPO$	Figure 9.b1- 9.b3

Table 1. Examples discussed in Patching Methods section.

PATCHING METHODS

The POs in Figure 5 can be patched using two separate approaches, which are outlined in this section. The simplest and straightforward method is to patch each pair of consecutive POs at a common perpendicular *x-crossing*. Assuming that both POs have the same x axis crossing ($y = 0, \dot{x} = 0$), only a $\Delta\dot{y}$ maneuver is required to transfer from one orbit to the other one. The process can be repeated to chain a sequence of multiple periodic orbits. Although ballistic transfers between a given PO sequence could exist, the nature of this method imposes a $\Delta\dot{y}$ cost. An alternative, more refined method, involves connecting PO sequences at a fixed Jacobi constant level, where ballistic transfers between POs are feasible. However, two periodic orbits with the same Jacobi constant cannot share a common perpendicular x-crossing. The PO sequences will therefore have x-crossing discontinuities, for which a differential corrector or an *optimizer* is used in order to generate a continuous trajectory. Alternatively, at an early design stage, the small discontinuities may be considered acceptable, similar to typical practice using the patched-conics model.

x-Crossing Patch Method

A planar x-axisymmetric PO is uniquely defined by two parameters at any of its two perpendicular x-crossings: $\{x, \dot{y}\}$ or $\{x, J\}$. A family of POs can be represented by a curve $\dot{y}$ vs. x, called the *characteristic curve*, or equivalently, by a curve J vs. x. To select the target periodic orbits of a given PO sequence, the characteristic curves of the families of two consecutive POs are used. The first PO is selected according to a target Jacobi constant, and is identified in its corresponding characteristic curve. The second PO is then selected to match the same x as the first PO, i.e. $x^+ = x^-$, where the $+$ and $-$ signs refer to the first and the second POs, respectively. The difference between $\dot{y}^-$ and $\dot{y}^+$, represents the cost of the transfer, such that $\Delta v = |\dot{y}^+ - \dot{y}^-|$.

Figure 6(a) shows the characteristic curves for the families LL_2 and Hb_2 (at the right x-crossing), used for the transfer $LL_2 \rightarrow Hb_2 \rightarrow DPO$ (Figure 5(a)). The families used here belong to the Jupiter/Europa system. In this example, the maneuver required to connect an LL_2 orbit with an Hb_2 orbit is approximately the same for all the values of Jacobi constants, $\sim \Delta v = 5m/s$. Following the same procedure, the families Hb_2 and DPO are patched together, to complete the transfer, this time, by using their left x-crossing. The transfer depicted in Figure 5(a) was designed at a Jacobi constant $J = 3.0018$. At this energy level, the cost to connect the orbits Hb_2 and DPO is $\sim \Delta v = 6m/s$; thus, the total cost of the entire transfer is $\Delta v = 11m/s$. For small values of the mass parameter μ (like the ones consider in this paper), transfers from LL_1 to DPO are approximately mirror images of the transfer LL_2 to DPO.

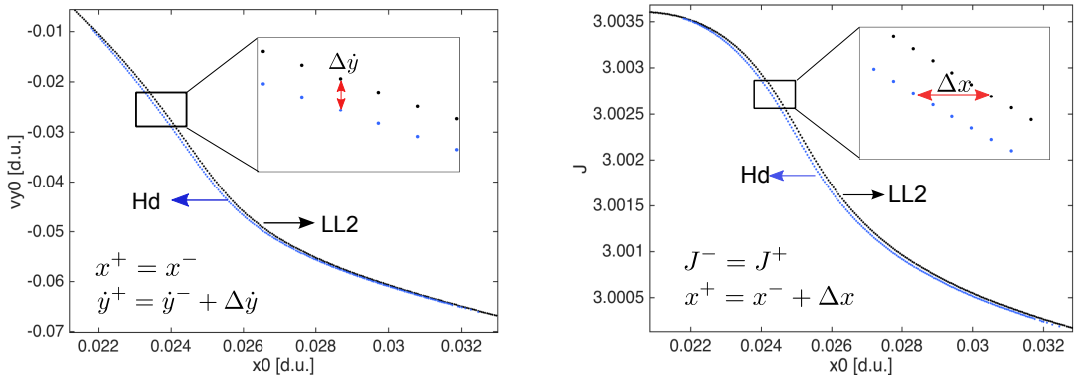

(a) x-crossing patch method

(b) Optimization method: POs at fixed J

Figure 6. Hb_2 and LL_2 families of Jupiter-Europa system. POs selection strategy for the two patching methods

Optimized Patch Method

A PO sequence can be used as an initial condition for an optimization procedure. If a ballistic transfers between unstable periodic orbits exists, the transition must occur at a fixed Jacobi constant. Hence, to use the *optimized patch method*, the periodic orbits of the desired sequence are therefore chosen by their Jacobi constant values. The POs selection is done by using the x vs J curves of adjacent POs, in a similar manner as in the x-crossing patch method; however, in this case, the consecutive POs are selected such that $J^+ = J^-$.

Figure 6(b) shows the curves for the families LL_2 and Hb_2, used for the transfer in Figure 5(a). It can be seen from the figure that an x discontinuity between the two target POs exits. For this particular example, the x discontinuity is $\sim 32km$. To create a continuous trajectory from the selected POs sequence, a differential corrector can be used, where a solution similar to the x-crossing patch method is expected. In examples presented in this paper, the connection is done by using a multi-shooting method and the software SNOPT. To reduce the sensitivity of the procedure, each periodic orbit is divided in multiple segments, allowing for intermediate maneuvers. The targeting points are the initial state of the first PO and the final state of the last PO, with constraints at the patch points. The implemented procedure is similar to the one used in Ref 10.

Figure 7 shows the trajectories associated to transfer $LL2$ to a DPO at three different Jacobi constants, where both the x-crossing patch method (a-c) and the optimized patch method (d-f) were used. The two solutions are practically identical, and only exhibit a small difference in the total cost of the transfer (Table 2). The optimization method converges to a quasi-ballistic solution ($\Delta v \lesssim 1m/s$). Even though the optimized patched method yields a lower cost solution, the difference in cost between the two methods is small. Hence, the simplicity of the x-crossing patch method makes it ideal for preliminary studies.

Special Case: Transfers to Prograde Orbits

The applicability of the x-crossing patch method depends on the Jacobi constant level and the specific PO sequence used. The connection between two POs is achieved at a low Δv cost only

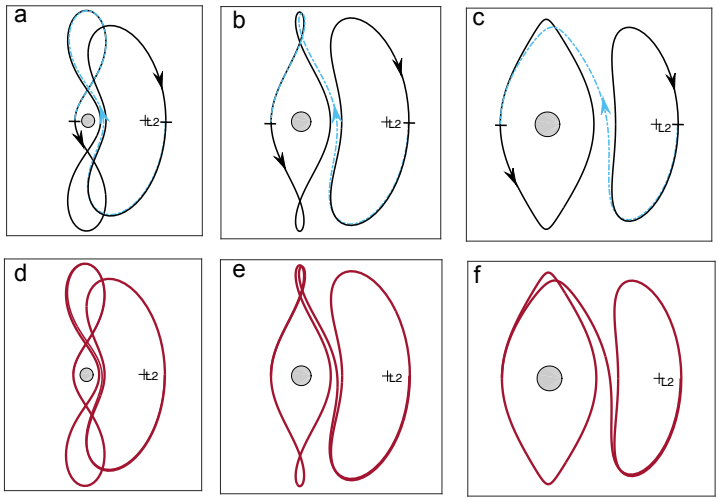

Figure 7. x-crossing patch method (upper row), optimized solution (lower row). $LL2$ **to** DPO **transfers: a) and d)** $J = 3.0010$**, b) and e)** $J = 3.0018$**, c) and f)** $J = 3.0025$**. Jupiter-Europa system (example 2).**

if the characteristic curves of both families lay close to each other (either along the entire family or in a specific range of Jacobi constants). In the case of the families LL_1 - Hg_n, and Hg_n- LL_2, this condition is satisfied. Hence, the families Hg_n are good approximations of the heteroclinic connections between LL_1 and LL_2 (Figure 4) at any Jacobi constant value between the low-energy regime.

Quasi-ballistic connections from/to prograde orbits via Hb_1 and Hb_2 exist at certain energy levels. Figure 8 shows the x vs J curves for the families DPO, LPO_2 and Hb_2 for the Jupiter-Europa system. At the energy levels corresponding to ($3.0000 < J < 3.0025$), the Hb_2 (blue) and DPO (black) families are very close to each other, indicating the existence of relatively inexpensive transfers between them. The solutions circled in red in Figures 8(a) and 8(b) that exist in this energy interval, are the POs used in the transfers depicted in Figure 7. Notice, that at the critical value ($\sim$ J=3.0025), the two families begin to diverge. In this case, the x-crossing patch method loses its applicability, resulting in expensive transfers.

The DPO family is highly unstable at low values of Jacobi constant (high energy). This instability quickly decreases as the Jacobi constant increases, reaching a critical value at $J = 3.0037$, where the family becomes stable, transitioning to the LPO_2 family (grey in Figure 8). In the interval ($3.0025 < J < 3.0037$), the perpendicular crossing of the DPO (black) and Hb_2 (blue) families are significantly separated, thus, the x-crossing patch method is not suitable in this interval. Despite the wide discontinuity, the optimized method in fact can still be used to achieve low cost transfers. Figure 8(b) shows the characteristic curve for families in this interval of energy that can be used to generate $LL_2 \rightarrow Hb_2 \rightarrow DPO$ transfers. The trajectories are shown in Figure 9(b) (initial guess in blue and converged solution in red) with optimized Δv in Table 2. Notice that multiple revs around the secondary necessary to obtain low cost transfers at this level of Jacobi constant due to the large state discontinuities at the initial guess.

The stability of the LPO_2 family makes transfers to and from this family expensive. This expense can be clearly seen in Figure 8(b), where the Hb_2 and LPO_2 families do not exist at the same

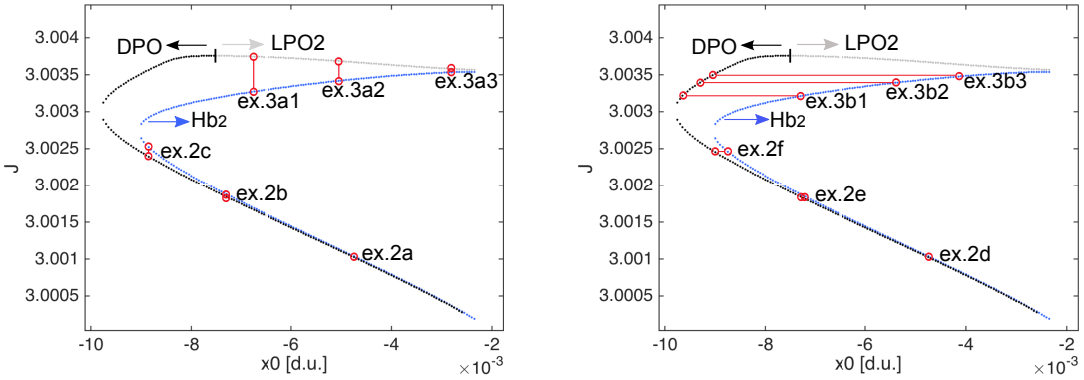

(a) x-crossing patch method

(b) POs at fixed Jacobi constant for optimization

Figure 8. Families DPO, LPO_2 and Hb_2, and POs selection for examples 2 and 3.

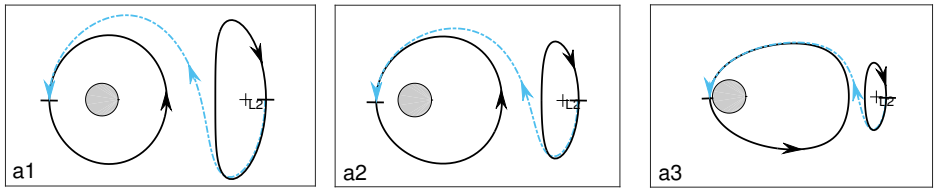

(a) $LL_2 \rightarrow Hb_2 \rightarrow LPO_{east}$. x-crossing patch method

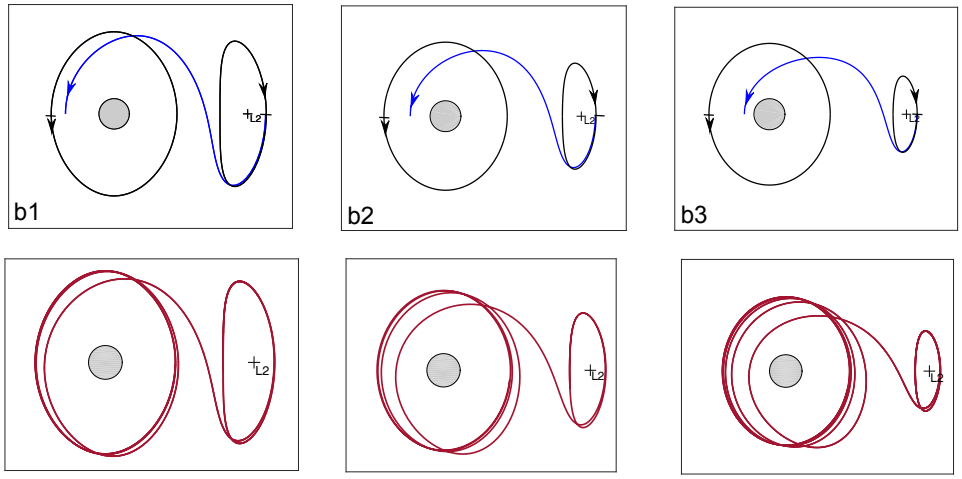

(b) $LL_2 \rightarrow Hb_2 \rightarrow DPO$. optimization method

Figure 9. Transitions from LL_2 to different prograde BPOs via Hb_2 family. (example 3)

Jacobi constant level. Therefore, the optimized patch method may not be suitable for these types of transfers. On the other hand, a transfer from Hb_2 to LPO_2 can be designed using the x-crossing

Example	J	Δv (m/s) x-patch	Δv (m/s) opt.	Example	J	Δv (m/s) x-patch	Δv (m/s) opt
ex. 1.a	3.0018	11	~ 1	ex. 3.a1	3.0032	45	-
ex. 1.b	3.0018	11	~ 1	ex. 3.a2	3.0034	25	-
ex. 1.c	3.0018	12	~ 1	ex. 3.a3	3.0035	7	-
ex. 2.a/d	3.0010	7	~ 1	ex. 3.b1	3.0032	-	1.5
ex. 2.b/e	3.0018	11	~ 1	ex. 3.b2	3.0034	-	2.5
ex. 2.c/f	3.0025	18	~ 1	ex. 3.b3	3.0035	-	3.5

Table 2. PPO sequences and Δv costs for the examples 1, 2 and 3.

patch method, since the families do overlap in x (Figure 8.a). Three examples are noted in this figure, ex. 3.a1, 3.a2, and 3.a3, with their corresponding converged trajectories in Figure 9.a. Note that in ex. 3a1, the Hb_2 and LPO_2 POs are significantly separated, and therefore require a large Δv to connect them. As the Jacobi constant increases, the Δvdecreases, until both POs families approach $J = 3.0035$. At this particular point, an accessible connection between the two families of only 2 m/s exists. This transfer provides important applicability for missions to the icy moons. For example, an orbiter placed in this low prograde orbit can provide long periods of visibility to the outer side of the moon, which can be used as relay orbit for a lander located on this side, or simply for observation and data collection. Additionally to the low cost of the transfer, placing and orbiter in a LPO requires little station keeping due to its stability. In the Applications section, it is shown that LPO_1 can be accessed at a similar cost by transitioning from LL_2 to LL_1 followed by a Hb_1 connection (Figure 14, example X).

ESCAPE/CAPTURE TRANSITIONS

Weak captures and escape trajectories are designed by using a group of POs that approximate heteroclinic connections between resonant orbits and secondary POs. Resonant periodic orbits are denoted as $R_{p:q}$, where p represents the number of revolutions of the spacecraft around the primary in a inertial frame in one period P_{sc}, and q is the number of revolutions of the secondary. In the rotating frame, p is observed as the number of petals of the periodic orbit (Figure 10). In the two-body problem (TBP) ,where the mass of the secondary is negligible, the period of one spacecraft revolution (T_p), and the period of the secondary (T_q) are related by integer numbers as $pT_p = qT_q$. However, in the CRTBP, when the gravity of the secondary is considered, the TBP periods are no longer related precisely by integers. Instead, the relation becomes an approximation, $pT_p \approx qT_q$.[27] The dimensionless period of the secondary T_q in the CRTBP is 2π, while $P_{sc} = pT_p$, thus, the resonant period can be approximated as $P_{sc} \approx 2\pi q$.

This approximation begins to fail as the particle has closer encounters with the secondary, and gets even worse when the particle loops around the weak stability zone during the encounters. Figure 10 shows an example of several 7:6 resonant orbits at the same Jacobi constant with different secondary approach geometries. Although they follow different paths in the vicinity of $B2$, resulting in different periods, the 7:6 structure around the primary remains approximately the same. Hence, the relationship between the periods T_p and T_q can be retrieved if one considers just the time required for the particle to leave and return the sphere of influence (SOI) of the secondary. Ref. 28 provides

a model to determine the type of CRTBP resonance that accounts for these time differences. In the present paper, a simpler approach, based on the osculating semi-major axis a of the periodic orbits with respect to respect to the primary is used.

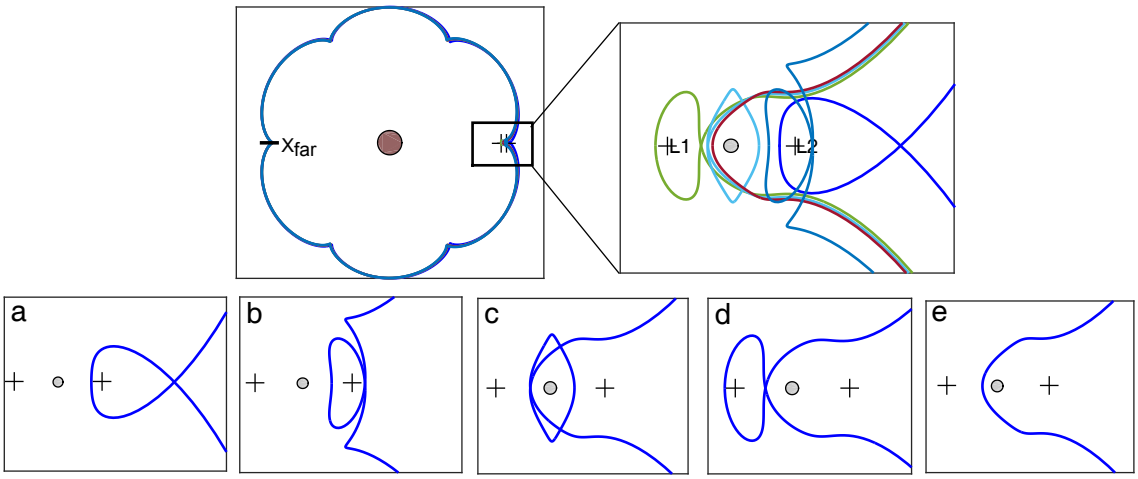

Figure 10. Sample of different 6:7 resonances. Families b, c, and d approximate heteroclinic connections with L2,DRO and L1, respectively

When far from the secondary, i.e. the negative x-crossing of the PO (x_{far} in Figure 10), the spacecraft trajectory is well approximated by a Keplerian arc.[29] Hence, the osculating a is approximately the same for all the PO families of the same resonance, and is very close to the two-body semi-major axis a_{TBP}, where $a_{TBP} = (p/q)^{2/3}$ in normalized units. Figure 11 (a) shows the different families of the 7:6 resonant trajectories, illustrating how all families of same resonance live in a band of a values, given by $a_{TBP} \pm \Delta a$, despite the significant differences between their periods (Figure 11 (b)). For Europa Δa is $1 \times 10^{-4} \times a_{TBP}$, while for Ganymede it is $3 \times 10^{-4} \times a_{TBP}$, and, in general, Δa is proportional to the mass parameter μ.

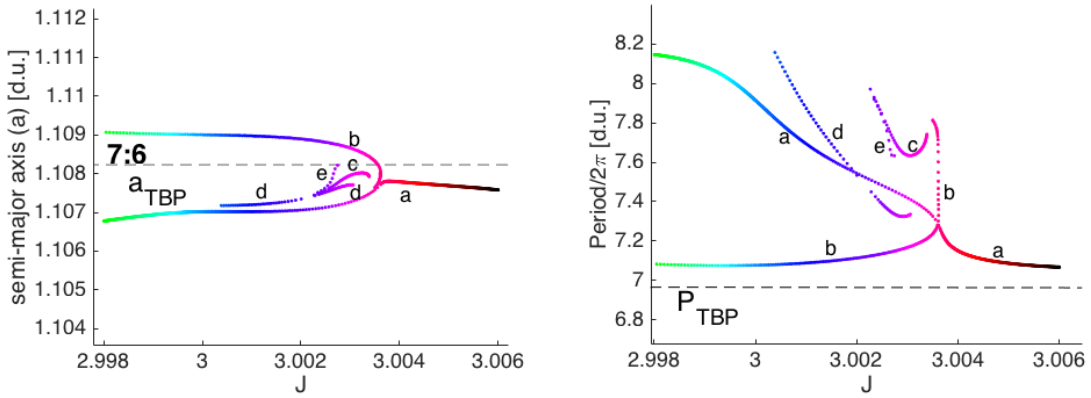

(a) Osculating semi-major axis map

(b) Period vs J map

Figure 11. Families of 7:6 resonances. Jupiter-Europa system.

From the families of outer resonances depicted in Figure 10, family a is referred to as a *simple* resonance, which is geometrically similar to a conic resonant in a rotating frame. Families b, c, and d approximate heteroclinic connections between $simple$ resonances and LL_2, DRO, and LL_1, respectively. We will define these types of POs as heteroclinic resonances, and represent them as $H_{p:q-PO}$, i.e. $H_{7:6-L2}$. Capture trajectories (and their symmetric departures) from inner or outer resonant orbits to secondary POs can be designed by using these special resonant families, and the Patched Periodic Orbits model is well-suited for the design. Figure 12 shows an example of a capture design using a 6:5 simple resonance and a LL_2 connected together with a heteroclinic resonance $H_{6:5-LL2}$. In a symbolic representation, the capture can be written as $R_{6:5} \rightarrow H_{6:5-LL_2} \rightarrow LL_2$.

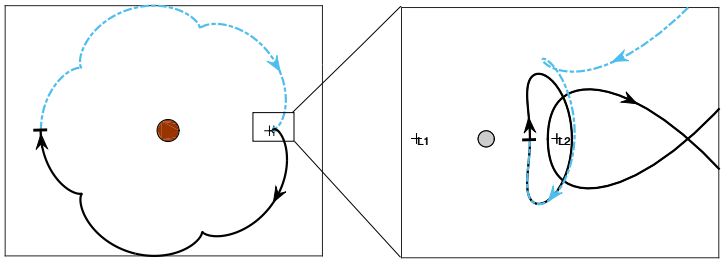

(a) PPO model: $R_{6:5} \rightarrow H_{6:5-LL2} \rightarrow LL2$

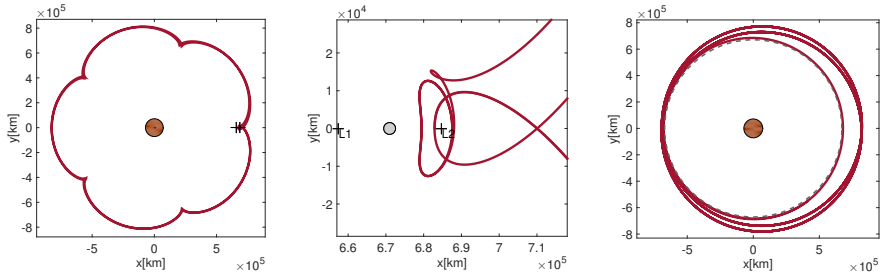

(b) Optimized solutions. Rotating and inertial frame

Figure 12. Capture design via Heteroclinic connection between $R_{6:5}$ and LL_2. Jupiter-Europa System, J=3.0025. (example 4)

The heteroclinic resonant families exist in a limited range of Jacobi Constant. The range at which they exist will define the energy level of the trajectory design or, in other words, a given Jacobi constant defines the resonances from which a capture is possible. Figure 13 shows families of $H_{p:q-LL_2}$ resonances for the Europa system, depicting the upper bound of the Jacobi constant for each resonance. For instance, a ballistic capture trajectory from a 7:6 resonance is possible around the entire low-energy regime, however, if the moon tour transfer ends in a 5:4 resonance, ballistic captures will be possible only below $\approx J = 3.0017$.

APPLICATIONS

The PPO model allows for several types of applications on low-energy transfer design. Some representative examples are presented here. Figure 14 shows different transfer trajectories from outer resonances to prograde orbits around Europa, at three different Jacobi constant levels. The capture

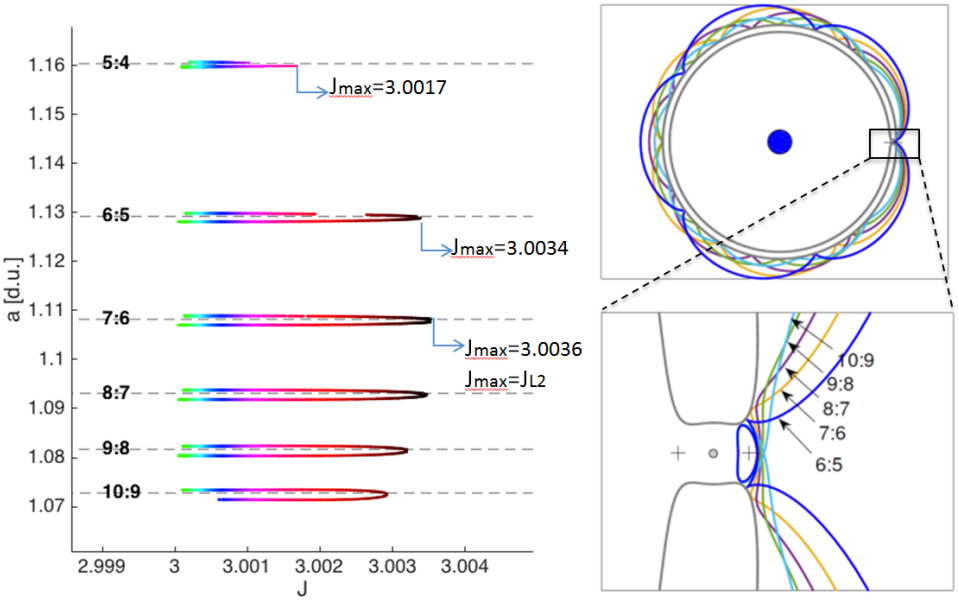

Figure 13. Families $H_{p:q-LL_2}$ for different p and q values. Osculating semi-major axis map. Energy coloured from low (dark) to high (light). Jupiter-Europa system.

transition is design by using heteroclinic resonances arriving at LL_2. In the Jupiter environment, the time of the transfer is critical due to the high radiation. Hence, low resonances (i.e. small values of q) are preferable. The $H_{p:q-LL_2}$ orbits are then chosen as the lower heteroclinic resonance at the specified Jacobi constant. Figures 14.a and 14.b, are transfer trajectories to DPOs from resonances 4:5 and 5:6, respectively. Figure 14.c shows a transfer from a 6:7 resonance to a LPO_2. In figures 14.d and 14.e, following from the resonant capture, two different transfers between LL_2 and LL_1 are shown, followed by a transfer to an LPO_1. In the example in Figure 14.e, the connection from LL_2 to LL_1 is a achieved via Hg_2, adding two revolutions around Europa during the transfer. This entire trajectory is easily constructed using the PO database and the PPO method, and can be represented by the POs sequence:

$$R_{6:7} \rightarrow H_{R6:7-LL2} \rightarrow LL_2 \rightarrow Hg_2 \rightarrow LL_1 \rightarrow Hb_1 \rightarrow LPO_1 \ \ \{J = 3.0035\}$$

Europa Lander and Orbiter: In this example, the objective is design a Europa mission, where a lander and an orbiter are sent together in a low energy tour, approaching Europa in a resonant capture to LL_2. With a small maneuver, both the lander and the orbiter can be separated into two different paths (Figure 15), the lander following a trajectory towards the surface of Europa, and the orbiter towards a Lyapunov orbit in the direction of the landing site, serving as a relay satellite. Due to the fact that Europa is tidally locked, an orbiter at L_1 provides continuous visibility over a station located in the inner side of the moon (sub-Jovian side). On the other hand, an orbiter at L_2, provides continuous coverage over the anti-jovian side of the moon.

There exists a PO sequence that allows to place both orbiter and lander in their respective target orbits at a small cost control. In this case, the extended BPO families Hm_1 and Hm_2, introduced in Figures 3.k and 3.l are utilized. The family (Hm_2) leaves from a L_2 Lyapunov orbit, approaching the Europa surface in retrograde motion at the sub-jovian side (Figure 15.b, black segment). The

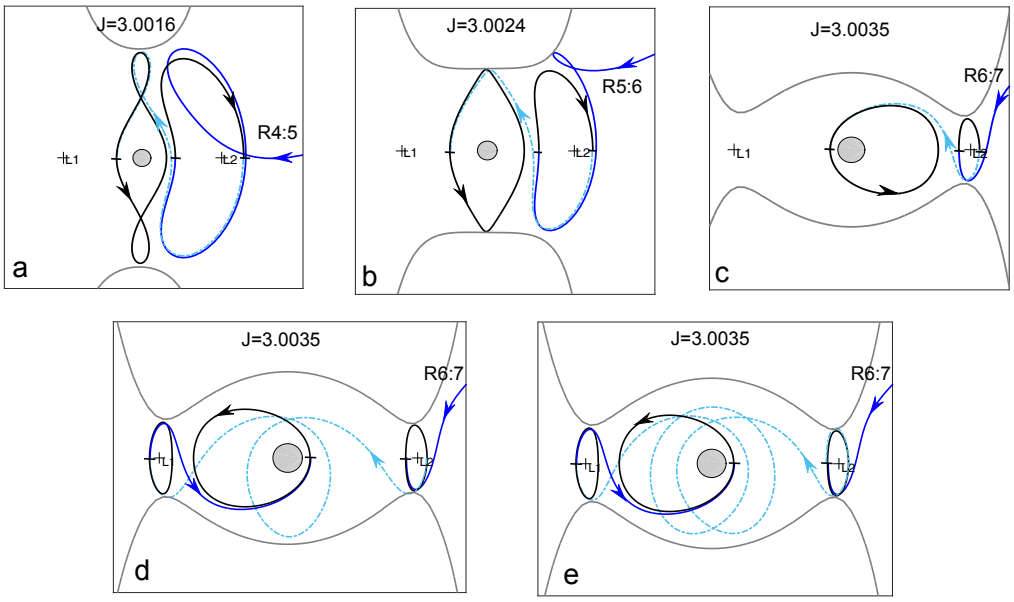

Figure 14. Europa captures. Transfers from outer resonances to DPO, LPO_1 and LPO_2. (example 5)

cost of the separation maneuver from the Lyapunov orbit is $\sim$ 2m/s. The orbiter, still at LL_2, can then follow the sequence $LL_2 \rightarrow Hg_0 \rightarrow LL_1$ to transfer to a final relay orbit at L_1 (Figure 15.a). The periodic orbit Hm_2 is the last Hm_2 family, ending when the left perpendicular x-crossing reaches the Europa surface. The Jacobi constant of this particular PO is $J = 3.0018$, defining the energy level of the transfer. At this energy level, the surface velocity of the lander is 1930 m/s, which defines the descending maneuver budget. The Jacobi constant also determines the minimum final resonance of the moon tour. At this Jacobi constant, quasi-ballistic captures exist from resonances 5:6, via $H_{R5:6-LL2}$ connections (Figure 13). Captures from resonances 4:5 are also possible at the cost of an additional maneuver. Figures 15.c and 15.d, show a similar lander-orbit trajectory design, targeting the anti-jovian side. The transfer cost are presented in Table 3. Notice that this trajectory is similar in structure as the ARTEMIS trajectory, known for the complexity of its design.

Two examples of a low energy transfer from outer to inner resonances around Ganymede, are presented in Figure 16. These trajectories can be used to connect the moon tour coming from Callisto in the course to Europa. In the first example, the transition from a 3:4 resonance to a 5:4 resonance is considered (Figure 16.a). The connection between LL_2 and LL_1, is performed by using a Hg_0 connection, providing a quick pass around Ganymede. In the second example (Figure 16.b), the LL_2 to LL_1 transition is performed throughout a Hg_4 connection, allowing multiple revs around Ganymede, and extended science collection. In the second example, the transfer is designed at a lower energy level, beginning in a 4:5 resonance. Both examples are optimized, converging on a transfer of $\sim$ 2 m/s (Table 3). These solutions, in practical sense, can be considered ballistic.

Conly-Moser Theorem. The resonant transition in the Jupiter/Ganymede system, depicted in Figure 16.b), was modified as an attempt to provide a numerical verification of the Conley-Moser theorem. In this exercise, multiple revs (10 at each pass) where allowed at each periodic orbit in

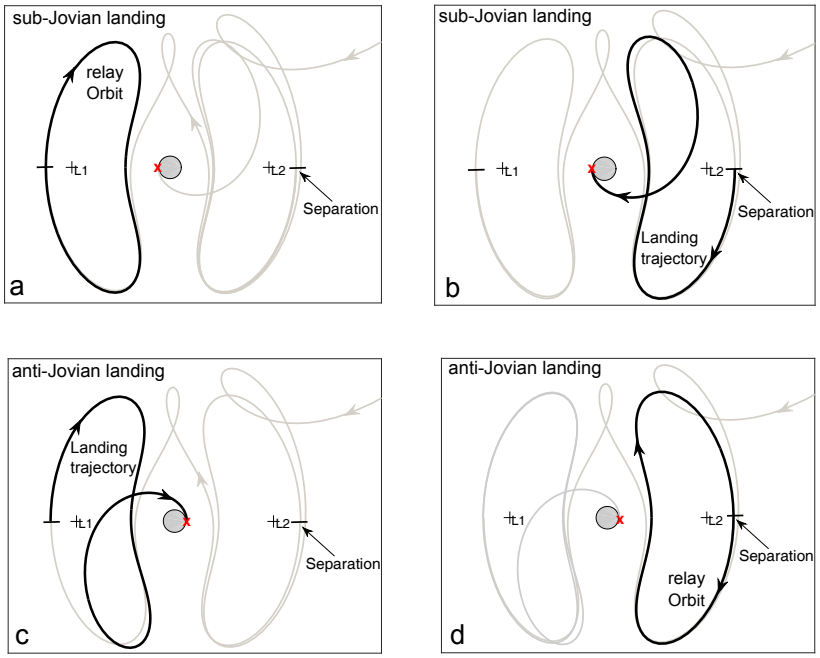

Figure 15. Europa lander-orbiter. a) and b): Sub-jovian landing site with a LL_1 relay orbit. c) and d): Anti-jovian landing site with a LL_2 relay orbit. (example 6)

the sequence, including 5 revs around Ganymede in the transition from L_2 to L_1. The optimization procedure resulted in a solution of similar cost as the original example. An indefinite number of revs around the resonant orbits and the Lyapunov orbits are possible, due to their periodicity. The succession of orbits Hb_n, with $n = 0, ..., 5$ presented in Figure 4 , suggests that similar orbits with an arbitrary number n can also exist, but its computation is restricted to the available machine precision.

Finally, two examples of captures around the Lagrangian points L_1 and L_2 of the Moon are presented (Figure 17). These examples, useful in the design of low energy Earth-Moon transfers, also show the extension of the PPO model applicability over higher values of mass parameters μ. The minimum inner resonance (i.e smaller semi-major axis) that exhibit heteroclinic connection with BPOs in the Earth-Moon system, is the 5:2 resonance.[17] The lower bound of the energy at which these connections exists is given by $J < J_{L1} = 3.188$. Figures 17(a) and 17(b) show a transfer from a 5:2 resonance to a LL_2 orbit, with a temporal capture around L_1. The POs sequence associated to this transfer is $H_{R5:2-LL1} \rightarrow LL_1 \rightarrow Hg_0 \rightarrow LL_2$ ($J = 3.12$). Once optimized (Figure 17(b)), this POs sequence produces a quasi-ballistic transfer that required a total maneuver of less than 1 m/s. Therefore, the cost of placing a station around L_1 or L_2, is given by the cost of reaching an Earth-Moon 5:2 resonant orbit. In Figure 17(a) the targeting initial state is denoted by $\mathbf{X}^*$, and has associated osculating semi-major axis $a = 0.5338$ (d.u.), and osculating eccentricity $e = 0.5231$. Figures 17(c) and 17(d) show a similar transfer connecting a 5:2 resonance with a LL_2 orbit, excluding the temporal capture around L_1. In this case, the Heteroclinic resonance $H_{R5:3-L2}$ was used. The total cost of a low energy Earth-Moon transfer can be benefit by this strategy. Furthermore, connecting these solutions with a lower resonance (i.g. 3:1) via resonant

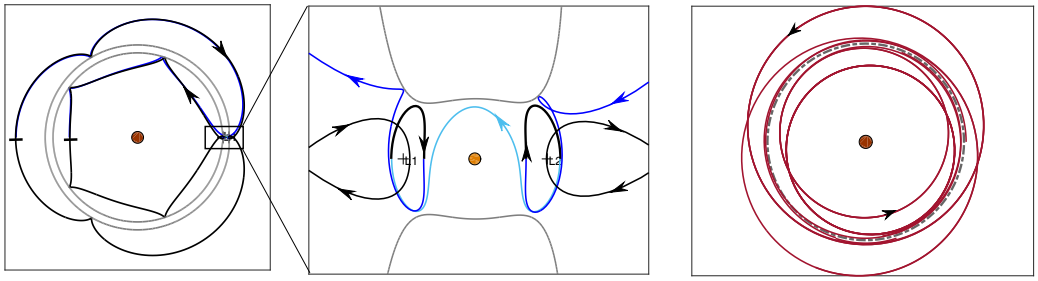

(a) R3:4 $\rightarrow$ R5:4. $L_2 1$ to L_2 transition via $HR0(J = 3.0060)$

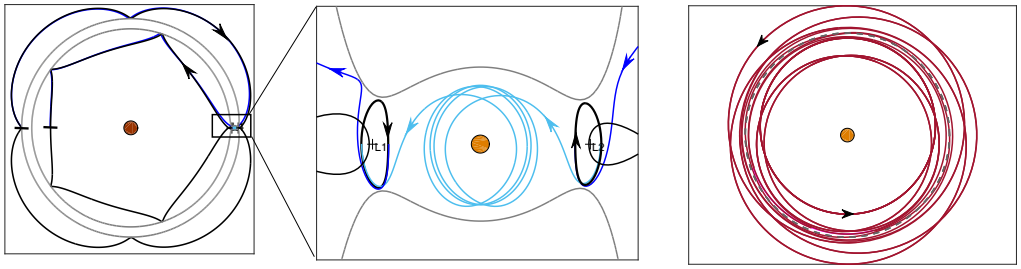

(b) R4:5 $\rightarrow$ R5:4 $L_2 1$ to L_2 transition via $HR4(J = 3.0072)$

Figure 16. Transitions from outer to inner resonances, Jupiter-Ganymede system. Left side: POs sequence (rotating frame). Right side: optimized solutions (inertial frame). (example 7)

hopping,[29] can lead to efficient low cost Earth-Moon transfers, and it is left for future work. Of course, the solutions presented in this paper are subject only to the dynamics of the CRTBP. Future work also includes transitioning these PPO solutions to ephemeris models.

CONCLUSIONS

The Patched Periodic Orbit (PPO) model has been introduced as a means to ease the complexity of designing low energy transfers. The PPO model is analogous to the patched conic model in the two-body problem, when conic segments are used as building blocks, which are patched together to give rise to full complex trajectories. In the PPO model, the building blocks are precomputed three-body periodic orbits (POs), which are then simply patched together to build transfer mechanisms in multi-body environments. A database of POs for a variety of three-body problems in the Solar System has been generated by the authors and is provided online. The database, together with the method, provides a framework for easily computing complex trajectories.

The PPO model focuses on the design of low energy transfer trajectories around the secondary, including quasi-ballistic captures and escape transitions to and from the vicinity of the secondary. Ballistic transfers between the libration points L_1 and L_2, and transitions into direct orbits are included as well. The computation of these inexpensive transfers has traditionally involved the computation of manifolds of unstable POs and their intersection. The PPO model replaces the need of this computational expensive task and therefore greatly reduces the complexity of the design of

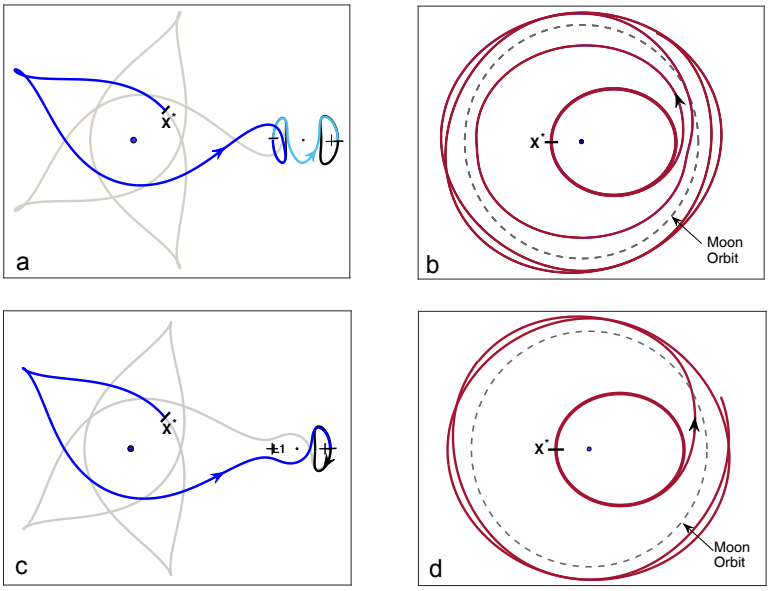

Figure 17. Earth-Mooon transfers. Left side figures: Patched Periodic Orbits model (rotational frame). Right side figures: Optimized sol. (Inertial Frame). (example 8)

Example	Figure	J	Δv (m/s)	Example	Figure	J	Δv (m/s)
ex. 4	13.b	3.0025	< 1	ex. 6	16.a-16.d	3.0017	< 3
ex. 5	15.a	3.0016	< 1	ex. 7	17.a	3.0060	< 2
ex. 5	15.b	3.0024	< 1	ex. 7	17.b	3.0072	< 2
ex. 5	15.c-15.e	3.0035	~ 8	ex. 8	18.b,18.d	3.1200	< 1

Table 3. Δv costs for the examples 4 to 8. (Optimized solutions)

low-energy transfer trajectories. Applications that would greatly benefit from this novel strategy are low-cost Earth-Moon transfers, libration point missions and moon tour designs. As an additional feature, it is shown how families of connecting resonances can be represented via maps as a visual tool to provide valuable dynamical insight into the systems, helping to quickly asses the type of connecting resonances at which capture/escape trajectories exist for any system, and their energy regimes.

REFERENCES

[1] W. S. Koon, M. W. Lo, J. E. Marsden, and S. D. Ross, "Heteroclinic Connections between Periodic Orbits and Resonance Transitions in Celestial Mechanics," *Chaos*, Vol. 10, June 2000, pp. 427–469.

[2] G. Gómez, W. S. Koon, M. W. Lo, J. E. Marsden, J. J. Masdemont, and S. D. Ross, "Connecting orbits and invariant manifolds in the spatial restricted three-body problem," *Nonlinearity*, Vol. 17, September 2004, pp. 1571–1606.

[3] E. Belbruno, *Capture Dynamics and Chaotic Motions in Celestial Mechanics*. Princeton, New Jersey: Princeton University Press, 2004.

[4] C. Conley, "Low energy transit orbits in the restricted three-body problem," *SIAM Journal on Applied Mathematics*, Vol. 16, July 1968, pp. 732–746.

[5] S. B. Broschart, M.-K. J. Chung, S. J. Hatch, J. H. Ma, T. H. Sweetser, S. S.Weinstein-Weiss, and V. Angelopoulos, "Preliminary trajectory design for the ARTEMIS lunar mission," AAS/AIAA*Astrodynamics Specialist Conference*, Pittsburgh, PA, August 2009.

[6] K. Howell, B. Barden, R. Wilson, and M. Lo, "Trajectory Design Using a Dynamical Systems Approach with Application to Genesis," AAS/AIAA*Astrodynamics Specialist Conf.*, Sun Valley, ID, August 1997.

[7] R. P. Russell and T. Lam, "Designing Ephemeris Capture Trajectories at Europa Using Unstable Periodic Orbits," *Journal of Guidance, Control, and Dynamics*, Vol. 30, March-April 2007.

[8] W. Koon, M. Lo, J. Marsden, and S. Ross, "Constructing a low energy transfer between Jovian Moons," *Contemporary Mathematics*, Vol. 292, 2002, pp. 129–145.

[9] G. Lantoine and R. P. Russell, "Near Ballistic Halo-to-Halo Transfers between Planetary Moons," *The Journal of the Astronautical Sciences*, Vol. 58, No. 3, 2011, pp. 335–363.

[10] G. Lantoine, R. P. Russell, and S. Campagnola, "Optimization of low-energy resonant hopping transfers between planetary moons," *Acta Astronautica*, Vol. 68, April-May 2011, pp. 1361–1378.

[11] S. Campagnola and R. P. Russell, "Endgame problem part 2: Multi-body technique and T-P graph," *Journal of Guidance, Control, and Dynamics*, Vol. 33, March-April 2010, pp. 476–486.

[12] R. L. Anderson and M. W. Lo, "Flyby Design using Heteroclinic and Homoclinic Connections of Unstable Resonant Orbits," AAS/AIAA*Space Flight Mechanics Meeting, No AAS 11-125*, New Orleans, LA, February 13-17 2011.

[13] R. L. Anderson and M. Lo, "Role of invariant manifolds in low-thrust trajectory design," *Journal of Guidance, Control, and Dynamics*, Vol. 32, 2009.

[14] S. Ross and D. J. Scheeres, "Multiple Gravity Assists, Capture, and Escape in the Restricted Three-body roblem," *SIAM Journal on Applied Dynamical Systems*, Vol. 6, No. 3, 2007, pp. 576–596.

[15] M. W. Lo and J. S. Parker., "Unstable resonant orbits near Earth and their Applications in Planetary Missions," AIAA/AAS *Conference*, Vol. 14, Providence, RI, August 2004.

[16] M. Lo, "The Interplanetary Superhighway and the Origins Program," *IEEE Aerospace 2002 Conference*, Big Sky, MT, March 2002.

[17] R. L. Restrepo and R. P. Russell, "A Database of Planar Axi-Symmetric Periodic Orbits for the Solar System," AAS/AIAA *Astrodynamics Specialist Conf, AAS 17-965*, Stevenson, WA, August 2017.

[18] V. Szebehely, *Theory of Orbits: The Restricted Problem of Three Bodies*. New York: Academic Press Inc., 1967.

[19] B. Barrabés, J. Mondelo, and M. Ollé, "Numerical Continuation of Families of Heteroclinic Connections Between Periodic Orbits in a Hamiltonian System," *Nonlinearity*, Vol. 26, 2013, pp. 274–2765.

[20] E. Canalias and J. J. Masdemont, "Homoclinic and heteroclinic transfer trajectories between planar Lyapunov orbits in the Sun-Earth and Earth-Moon systems," *Discrete and Continuous Dynamical Systems*, Vol. 14, 2006, pp. 261–279.

[21] C. Zagouras and V. Markellos, "Axi-symmetric Periodic Orbits of the Restricted Problem in Three Dimensions," *Astronomy and Astrophysics*, Vol. 59, 1977, pp. 79–89.

[22] J. S. Parker, K. E. Davis, and G. H. Born, "Chaining Periodic Three-Body Orbits in the Earth-Moon System," *Acta Astronautica*, Vol. 67, 2010, pp. 623–638.

[23] I. A. Robin and V. V. Markellos, "Numerical determination of three-dimensional periodic orbits generated from vertical self-resonant satellite orbits," *Celestial Mechanics*, Vol. 4, 1980, pp. 395–434.

[24] R. Broucke, "Periodic Orbits in the Restricted Three-Body with Earth–Moon Masses," Tech. Rep. 32-1168, Jet Propulsion Laboratory, California Institute of Technology, 1968.

[25] M. Lara and R. P. Russell, "On the Family *g* of the Restricted Three-Body Problem," *Monografías de la Real Academia de Ciencias de Zaragoza*, Vol. 30, 2007, pp. 51–66.

[26] M. Hénon, "New Families of Periodic Orbits in Hill's Problem of Three Bodies," *Celestial Mechanics and Dynamical Astronomy*, Vol. 85, No. 3, 2003, pp. 223–246.

[27] C. Murray and S. Dermott, *Solar System Dynamics*. Cambridge: Cambridge University Press, 1999.

[28] B. Barrabés and G. Gómez, "Spatial p-q resonant orbits of the RTBP," *Celestial Mechanics and Dynamical Astronomy*, Vol. 84, 2002, pp. 387–407.

[29] S. Campagnola, P. Skerritt, and R. P. Russell, "Flybys in the planar, circular, restricted, three-body problem.," *Celest. Mech. Dyn. Astr.*, Vol. 113, June 2012, pp. 343–368.